Tellus (2000), 52A, 93–108

TELLUS
ISSN 0280–6495

Modeling the evolution of snow, snow ice and ice in the Baltic Sea

By TUOMO M. SALORANTA,* *Department of Geophysics, University of Helsinki, Finland*

(Manuscript received 12 October 1998; in final form 4 June 1999)

ABSTRACT

A numerical 1-dimensional fine grid sea ice thermodynamic model is constructed accounting specially for: (1) slush formation via flooding and percolation of rain- and snow meltwater, (2) the consequent snow ice formation via slush freezing, and (3) the effects of snow compaction on heat diffusion in snow cover. The model simulations from ice winter period 1979–90 are viewed against corresponding observations at the Kemi fast ice station (65°39.8′N, 24°31.4′E). The 11-year averaged model results show good overall consistency with corresponding total ice thickness observations. The model slightly overestimates the snow ice thickness and underestimates the snow thickness in February and March, which is mainly addressed to the model assumption of isostatic balance (i.e., slush formation via flooding), which was probably not fully satisfied at the coastal Kemi fast ice station. Supposing that this assumption is nevertheless generally valid away from the very coastal fast ice zone, an estimate for sea ice sensitivity to changes in winter precipitation rate is produced. Increased precipitation leads to an increase only in snow ice thickness with little change in total ice thickness, while a reduction in precipitation of more than −50% causes a significant increase in total ice thickness. The difference in modeled total ice thickness for the case of artificially neglecting snow ice physics is about 25%, which indicates the importance of including snow ice physics in a sea ice model dealing with the seasonal sea ice zone.

1. Introduction

The presence of the sea ice cover is a remarkable thing in nature in many ways. Sea ice forms a solid, thin and more or less white cover over the sea. It plays an important rôle in local and global weather and climate. This is mainly because of its physical nature as a good insulating medium between the ocean and atmosphere, and its high albedo. Sea ice also affects the salinity of the ocean surface layer, and thus the thermohaline convection. The hazards of sea ice for constructions and marine traffic contrasts with its possibilities for use as a platform for variable kind of activities, from on-ice traffic to leisure ice fishing. For organisms such as ice algae, some zooplankton species and the polar bear, sea ice is an essential environment for living and grazing.

Snow usually accumulates rapidly on sea ice after ice formation. This has a great effect on sea ice evolution and introduces significant modifications to exchanges of heat, momentum, salt and freshwater between the ocean–ice–atmosphere system. Snow metamorphism (compaction and freeze–thaw cycles) in snowpack will constantly change the properties of snow. This affects, among others, the thermal diffusivity and thickness of snow cover and consequently the ice thickness evolution.

The classical numerical sea ice models (Maykut and Untersteiner, 1971; Semtner, 1976; Gabison, 1987) treated the snow layer on the ice mainly as a factor that firstly reduces the ice growth rate and

* Present address: Geophysical Institute, Allegt. 70, 5007 Bergen, Norway.
E-mail: Tuomo.Saloranta@gfi.uib.no.

thus ice thickness due to its strong thermal insulating effect, and secondly delays the ice-melting season because it buffers the ice against solar radiation and surface melting.

However, observations from, e.g., Baltic and Antarctic seasonal sea ice zones (where snowfall is generally higher than in the Arctic) have shown that the traditional treatment of snow in ice models is not always sufficient to properly describe the real situation (Leppäranta, 1983; Crocker and Wadhams, 1989). The effect of snow in the seasonal sea ice zone can be very different from its effect in the multi-year ice zone. For example, a relatively thin ice thickness together with heavy snow load can cause seawater flooding at the ice–snow interface, or a mild period with rainfall cause wetting of snow, both which lead to slush layer formation. The possible freezing of this slush, the so-called *snow ice formation*, must be then taken into account in ice growth calculations.

Snow ice formation is not only limited to sea ice. The existence of snow ice in subarctic lakes is common (Seinä and Kalliosaari, 1991; Gow and Govoni, 1983).

In the Baltic Sea snow ice usually forms some 10–30% of the total ice thickness (Palosuo, 1963; Seinä and Kalliosaari, 1991). In Antarctica, after the sea ice cover has been formed through the "pancake cycle" (Weeks, 1998), little congelation ice growth actually takes place due to high oceanic heat flux. The formation of snow ice via flooding can thus turn to be important (Ackley et al., 1990; Lange et al., 1990; Adolphs, 1998).

Snow ice can also play an important, but presently neglected rôle in the model simulations of climate and climate change (Fichefet and Morales Maqueda, 1997). Warmer climate together with increased precipitation may not lead to significant changes in the ice cover due to the greater portion of snow ice forming under these conditions (Ackley et al., 1990).

Sea water flooding can bring suspended nutrients and algae seed populations to the higher light levels at the ice surface, which can lead to a bloom condition on the top surface of the ice earlier in the spring season than can occur either under or within the ice cover (Ackley, 1986). The dielectric properties of sea ice surface are also changed by slush formation. This has important implications in SAR and microwave remote sensing.

Despite its potential importance, most of the published sea ice models do not include sophisticated and physically realistic treatment of the complicated role of snow in ice thickness evolution. For example, while neglecting snow ice formation in a model, one might have reproduced correct total ice thickness but in an unrealistic way, if snow ice component is locally significant. In this study, a 1-dimensional fine grid numerical thermodynamic model for sea ice is developed specifically focussing on snow effects, namely:

- the formation of slush and snow ice both by flooding snowpack, and due to percolation of rain and snow surface meltwater.
- snowpack evolution and metamorphism, especially compaction of snow and its effects on the thermal diffusivity of snow.

To produce the model results presented in Section 4, 11 ice winters (1979–90) at the Kemi fast ice station (65° 39.8′N, 24° 31.4′E) (Fig. 1), in the northern corner of Bay of Bothnia, are simulated and results are compared to observations. The sensitivity of northern Baltic sea ice to changes in snowfall as well as the errors produced by neglecting snow ice formation in an ice model is also studied.

2. Physics

2.1. The influence of snow on sea ice thermodynamics

The initial stage of the snow cover depends on the wind conditions and the crystal shape of the

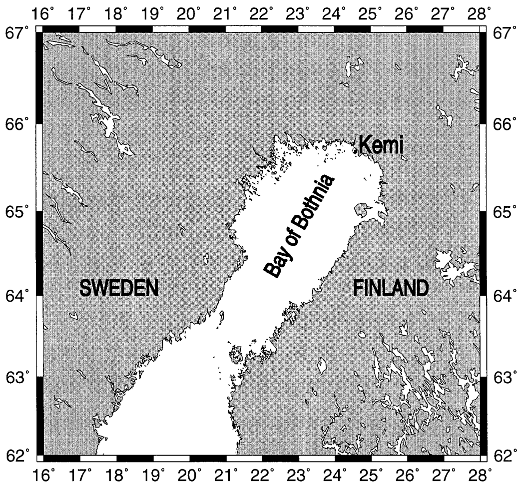

Fig. 1. Location of Kemi ice station (65° 39.8′N, 24° 31.4′E) in the northern corner of Bay of Bothnia.

snowflakes. The density of a new snow cover can vary over a large range, from $10\,\mathrm{kg\,m^{-3}}$ to $500\,\mathrm{kg\,m^{-3}}$ (Male, 1980). When snowfall has deposited on existing ice cover it has many different consequences. The low thermal conductivity of snow (insulation effect) leads to warmer ice temperatures in wintertime, which reduces the ice growth rate, and also "softens" the ice due to the increase in ice brine volume.

The thermal diffusion process in snow is much more complicated than in ice because several different mechanisms are present. In snow, heat can be transferred through the interconnected ice grains by conduction, across the air space by convection and radiation, and by the movement and phase changes of water vapor. The effective thermal conductivity of snow can vary by an order of magnitude with changing snow properties (density, grain size, etc.) — to illustrate the general effect, 10 cm of newly fallen snow can have the same insulation effect as 1 m of sea ice.

In contrast to the insulation effect reducing the ice thickness, the high albedo and light extinction of snow shields the ice in the melt season from solar radiation and protects it from melting (snow has to melt first before ice surface melting can really start).

The overload of snow on the ice cover can induce seawater flooding on the ice and thus formation of a water-soaked snow layer, i.e., a slush layer, which under negative air temperatures is frozen into snow ice. This superimposed ice growth can contribute significantly to the total ice thickness. Snow ice formation is a sink for the snow cover reducing its thickness, and this consequently diminishes the snow cover insulation, which favors further congelation ice growth. However, if unfrozen slush is present at the top of the ice it buffers the ice surface temperature to the freezing point temperature of the slush so that the underlying ice relatively soon, depending on its thermal inertia, becomes nearly isothermal and bottom melting due to oceanic heat flux may better reduce ice thickness. It is uncertain to what extent the higher salinity, and thus lower freezing point, of the slush can contribute to maintaining a significant temperature gradient at the bottom of the ice.

2.2. *Snow cover evolution*

Several factors can change an existing snow cover. Wind redistributes the snow cover forming greatly variable snow layer thickness from bare ice to enough to trigger flooding. Ice ridges and other irregularities in the ice field can act as obstacles for the wind field and greatly affect the snow accumulation pattern (Granberg, 1998). Open water, e.g., in leads, is a sink for drifting snow (Eicken et al., 1994). Evaporation from snow cover, as well as mass gain by sublimation (Granberg, 1998) can change significantly snow cover mass.

From the moment of deposition the snow cover begins to undergo metamorphic processes that change its properties constantly (Granberg, 1998). Snowpack can deform very rapidly especially during the snow melt season and due to rainfall. The percolating water in the snowpack can refreeze deeper in the snow forming ice lenses and other relatively impermeable layers in the snowpack, or contribute to a slush layer on ice.

2.3. *Slush and snow ice formation*

Ice cover serves as a buoyant platform on which snow cover accumulates. When the weight of the overlying snow cover exceeds the local buoyancy capacity of the ice, the ice surface (assuming level surface, i.e., no ridges) sinks beneath the waterline and seawater floods the ice mixing with snow, finally forming a slush layer. Here it is assumed that the ice is able to float isostatically and that some waterways for flooding are available. Otherwise an additional water overpressure exists under the ice.

With the two assumptions above, the buoyancy force that ice feels (per unit area) is in balance equal to the weight of the whole ice and snow layers (per unit area):

$$\rho_w H_{dr} = \rho_i^* H_i^* + \rho_s h_s, \tag{1}$$

where H_{dr} is ice draft thickness, H_i^* total ice column thickness including ice, snow ice and slush layers, h_s is snow thickness, ρ_w is sea water density, and ρ_s and ρ_i^* mean snow and total ice column densities.

Negative freeboards ($H_{dr} > H_i^*$) in eq. (1) lead to flooding and the balance between the buyoancy and gravitational forces is achieved again. The new slush formed in a flooding event is a sink for the overburden weight of snow and a (small) source for the buoyancy force in the form of slush.

Once the snow layer is soaked with water, some capillary suction probably exists so that the slush layer can actually be thicker than given by the balance eq. (1). The proper calculation of the capillary suction in snow requires information on the snow grain and void size, and their distribution (Pfeffer et al., 1990). Counteracting capillarity is the compaction of snow cover due to the presence of high concentrations of liquid water, which can reduce the thickness as well as the water content of the slush.

The waterways needed for flooding can be thermal cracks, holes, brine or other intercrystalline channels in the ice, or the ice edges (Röthlisberger, 1983). Little experimental data exists on how the water is then spread further on to the ice and by what speed. Sea ice does not usually crack under thermally induced stress, so water seeping via brine channels can play a very important role in the flooding phenomena (Crocker and Wadhams, 1989). The transition temperature between interconnected and discontinuous brine channels is highly dependent on the salinity and crystal structure of the ice (Eicken et al., 1995; Crocker and Wadhams, 1989).

Several observations show that flooding occurs in more or less discrete events and that there can be a significant time-delay (order of days or weeks) from the beginning of negative ice freeboard conditions to the balance conditions being restored (Röthlisberger, 1983; Crocker and Wadhams, 1989). Fig. 2 shows calculated potential flooding

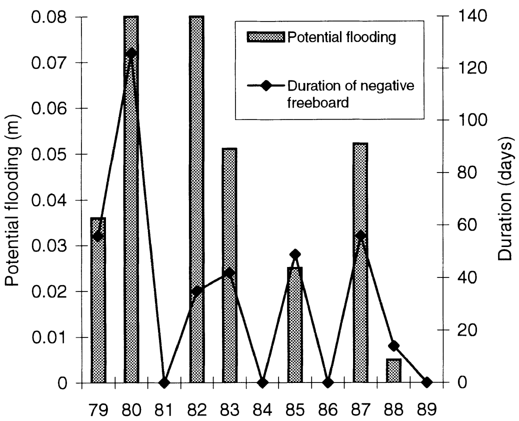

Fig. 2. Estimated potential flooding and duration of negative freeboard conditions at Kemi ice station 1979–90. Bulk snow density is assumed to be 200 kg m^{-3} and the density of water-soaked snow 450 kg m^{-3}.

and duration of the negative freeboard conditions at coastal Kemi fast ice station over the period 1979–90. These values are calculated from ice and snow thickness observations, applying eq. (14) and assuming a relatively low bulk snow density of 200 kg m^{-3} and a density of water-soaked snow of 450 kg m^{-3}. Some of the negative freeboard conditions in these estimations last for up to months, which indicates that sea ice in Kemi ice station could remain essentially in slight isostatic imbalance for a long time — even despite the hole drilled by the observer, it seems.

Flooding, together with percolation of melt- and rainwater are probably the main processes in slush layer formation, but brine expulsion and capillary suction of seawater through cracks in the ice may also contribute, as discussed in Adolphs (1998). The factors that can diminish the water content of the slush layer are evaporation, draining to sea and to melt ponds, and freezing into snow ice. The relative importance of these processes that control the slush layer water balance is poorly documented and is in addition expected to vary between fast ice zone and an ice field consisting of ice floes, mainly due to the difference in available waterways for flooding.

Slush itself is a mixture of water, ice and air bubbles. Its density is rarely measured in the field. Because slush density also is hard to measure accurately, Adolphs (1998) assumed that his highest measured values of 700 kg m^{-3} represented only the lower limit. He calculated theoretically the upper limit of 960 kg m^{-3} assuming no air bubbles in the slush.

The slush layer can freeze both from the top and the bottom, and it is not uncommon to find "sandwiched" layers of snow ice and slush or brine in the ice column (Gow and Gowoni, 1983). Bottom freezing is continued as long as the ice can serve as a heat sink. In top freezing, the latent heat of freezing must be conducted only through the snow layer, not through the ice and snow layers as in congelation ice growth. Slush already contains some ice originating from snow and it undergoes small volume expansion when it is frozen. This is why snow ice formation is a more effective way to produce new ice.

Crocker and Wadhams (1989) proposed in their Antarctic fast-ice model assumptions that the amount of latent heat released in the slush freezing process would be small and that most of the solidification of slush to snow ice was caused by the compaction of slush and drainage of the interstitial fluid.

The physical properties of snow ice differ from those of congelation ice. The crystal structure of first-year snow ice can be described as polygonal granular ice with isometric grain shapes and planar boundaries meeting at 120° (Eicken and Lange, 1989). Brine inclusions are typically spherical droplets at grain junctions (Eicken and Lange, 1989). Snow ice includes more air bubbles and is very distinctive from the coarser columnar crystal structure of congelation ice. However it is difficult to distinguish between frazil ice and snow ice crystal structure.

Palosuo (1965) measured snow ice densities between 860 and 890 kg m^{-3} in the Baltic Sea. Crocker and Wadhams (1989) used a value of 820 kg m^{-3} in their study, corresponding to an air bubble content of 10%. The thermal conductivity of the snow ice was taken to be $1/2\kappa_i$ (where κ_i is the thermal conductivity of ice) in the model study of Leppäranta (1983), while Crocker and Wadhams (1989) used equations for the thermal conductivity of bubbly, saline ice, and set κ_{si} to be $0.9\kappa_i$. The mechanical properties of snow ice are also quite different from that of congelation ice, snow ice being much weaker.

2.4. *Snow ice in sea ice models*

Among the few existing model studies on the role of snow ice in the Baltic Sea is the study of Leppäranta (1983). He included simple snowpack metamorphism and snow ice formation in his ice model, and concluded the importance of snow ice, and that in future sea ice models the packing of snow should be formulated as a function of weather conditions because of its importance to sea ice growth.

The Weddell Sea model study of Eicken et al. (1995) showed that increased snow ice formation and reduced short wave radiation absorption at the surface were not sufficient to balance the enhanced thermal insulation effect under increased snow precipitation. However, they also concluded that the combination of timing of snow accumulation, the permeability of the underlying ice and the change in heat flux at the surface produce a highly non-linear response in the ice to changes in snow boundary conditions.

Crocker and Wadhams (1989) modified Semtner's simplified 1-layer ice model (Semtner, 1976) for applying to snow- and platelet ice formation phenomena at McMurdo Sound, Antarctica. In their multi-year model runs they found that after the equilibrium cycle was reached after 5 model years, snow ice contributed 25% to total ice thickness at the end of winter and 100% at the end of summer when the ice thickness was in its minimum. The latter was found to be consistent with observations of characteristic Antarctic summer sea ice conditions, namely the absence of surface melting due to the relatively strong, cold and dry winds.

3. Model description

3.1. *Model equations*

The fundamental basis of the model is the 1-dimensional heat diffusion equation applied to ice, snow ice and snow (not applied to slush which is assumed to be isothermal):

$$\rho c \frac{\partial T}{\partial t} = \frac{\partial}{\partial z}\left(\kappa \frac{\partial T}{\partial z}\right) + d, \tag{2}$$

where ρc is heat capacity, T is temperature, κ is heat conduction coefficient and d is a source term (solar radiation). To determine the 2 boundary conditions needed for the solution with snow and ice layers, the following assumptions are used (S denotes salinity):

- The temperature at the ice–seawater interface must be at the freezing point $T = T_f(S)$.
- The temperature at the ice–snow interface is known either due to the presence of slush ($T = T_f(S)$) or otherwise it is derived from the continuity of the heat fluxes at the interface, where a strong discontinuity in thermal diffusivity exists (internal flux boundary condition, eq. (10)).
- The surface temperature is determined by an iteration process from the balance of the surface heat fluxes (flux boundary condition, eq. (7)).

Ice accretion or melting is possible at the bottom (congelation ice growth and bottom melting) and at the top (snow ice growth and surface melting) of the ice layer. The amount of freezing or melting at the ice bottom is calculated from the net heat flux between the oceanic heat flux (Q_w) and conductive heat flux at the bottom surface. Ice top surface freezing (snow ice formation) is calculated from the conductive heat fluxes to atmosphere through the snow pack and to underlying ice. Surface melting is triggered whenever the surface temperature is at the melting point, and the net surface heat flux determines the rate of melting.

The formulation of the surface heat fluxes in the model are (here the fluxes towards the surface are positive):

$$Q_h = \rho_a c_a C_h (T_a - T_0) U, \tag{3}$$

$$Q_e = L_e \rho_a C_e (q_a - q_0) U, \tag{4}$$

$$Q_r = S_{surf}(1-\alpha)(1-i_0), \tag{5}$$

$$Q_l = \varepsilon\sigma(T_a^4(a + b\sqrt{e})(1 + cN^2) - T_0^4), \tag{6}$$

$$\sum Q = Q_r + Q_l + Q_h + Q_e + \kappa \left.\frac{\partial T}{\partial z}\right|_{surf} = 0, \quad T < T_f, \tag{7}$$

where Q_h is the sensible heat flux, Q_e the latent heat flux, Q_r the net short wave radiation, Q_l the net long-wave radiation and $\sum Q$ is the total heat flux at the surface; ρ_a is the density of air, c_a is the specific heat of air, C_h and C_e are the turbulent exchange coefficients, L_e is latent heat of evaporation, T is temperature and q is specific humidity (subscripts a and 0 indicate atmospheric and surface values, respectively) and U is wind speed. The incoming short-wave radiation flux over the surface (S_{surf}) is a function of the solar constant (S_0), the eccentricity of earth's orbit around the sun (E), solar altitude in degrees (h), atmospheric turbidity (τ), atmospheric transmission and absorption (formulated by $\sin(h)$), and cloud correction ($f_c(N, h)$) where N is cloudiness (Iqbal, 1983; Reed, 1977):

$$S_{surf} = S_0 E \sin(h)\tau \sin(h) f_c(N, h), \tag{8}$$

$$f_c(N, h) = \begin{cases} 1 - 0.62N + 0.0019h, & N > 0.2 \\ 1 \qquad , & N \leqslant 0.2. \end{cases} \tag{9}$$

The short-wave energy flux available to the ice or snow surface is further controlled by albedo (α) and i_0, which denotes the part of the solar radiation that penetrates under the surface layer ($z > 0.1$ m). The net long wave radiation flux is calculated as in Omstedt (1990) where ε is water surface emissivity, σ is Stefan–Boltzmann constant, e is air water vapor pressure, N is cloudiness and a, b and c are empirical constants equal to 0.68, 0.0036 and 0.18, respectively.

The ice–snow interface temperature is calculated as in Maykut and Untersteiner (1971) from the continuity of the heat fluxes at the interface:

$$\kappa_i \left.\frac{\partial T}{\partial z}\right|_{z=+0} = \kappa_s \left.\frac{\partial T}{\partial z}\right|_{z=-0}. \tag{10}$$

The specific heat and thermal conductivity of ice and snow ice are kept constant in the model. The thermal conductivity for low salinity ice is taken to be equal to that for fresh water ice (Yen, 1981), while the value for snow ice is adopted from Leppäranta (1983) (Table 1). The thermal conductivity of snow is formulated after Yen (1981):

$$\kappa_s = 2.22362(\rho_s)^{1.885}, \tag{11}$$

where κ_s is in W m^{-1} K^{-1} and ρ_s is expressed in units of g cm^{-3}.

The initial snow density is set to 225 kg m^{-3}. When slush formation is taking place, the density of the water-soaked snow is assumed to rise to 450 kg m^{-3} due to snow compaction.

The value for snow ice density is taken as a mean from the measured range of Palosuo (1965). Slush density is then estimated assuming: (1) the same air bubble content as the snow ice density indicates (4%), (2) a volume ratio of 49% ice and 47% water in the slush corresponding to the chosen water-soaked snow density and assuming no snow melting in slush formation, and (3) a 5% volume expansion when slush is freezing (for values, see Table 1).

Surface albedo is defined as a constant value for 4 different surface conditions: dry snow, wet snow, dry ice and melting (ponded) ice (Perovich, 1998) (Table 1). The parameter i_0 for the percentage of penetrating short-wave radiation into snow is kept zero, and i_0 for ice is calculated linearly as a function of cloudiness between the values of i_0 for clear and cloudy conditions (Grenfell and Maykut, 1977):

$$i_0 = 0.18(1 - N) + 0.35N. \tag{12}$$

3.2. *Numerical realization*

The model algorithm is briefly described:

1. Read meteorological forcing data from input file.

Table 1. *The main normal case model parameters*

Parameter	Symbol and value	Source
model timestep	$dt = 1.0$ h	
density of new snow	$\rho_{new\ snow} = 225$ kg m^{-3}	
seawater density	$\rho_w = 1000$ kg m^{-3}	
ice density	$\rho_i = 910$ kg m^{-3}	Crocker and Wadhams (1989); Szilder and Lozowski (1989)
snow ice density	$\rho_{si} = 875$ kg m^{-3}	Palosuo (1965)
slush density	$\rho_{slush} = 920$ kg m^{-3}	
snow compaction coefficients	$C_1 = 7.0$ m^{-1} h^{-1}	
	$C_2 = 21.0$ cm^3 g^{-1}	Yen (1981)
oceanic heat flux	$Q_w = 5$ W m^{-2}	
grid size	$dz_{ice} = 0.10$ m	
	$dz_{snow} = 0.03$ m	
thermal conductivity of ice	$\kappa_i = 2.09$ W m^{-1} K^{-1}	Yen (1981)
thermal conduct. of snow ice	$\kappa_{si} = 0.5\kappa_i$	Leppäranta (1983)
specific heat of ice	$c = 2114.0$ J kg^{-1} K^{-1}	Yen (1981)
latent heat of freezing of ice	$L = 333\,500$ J kg^{-1}	Yen (1981)
ice salinity	$S_i = 1.0$ psu	Palosuo (1963)
air–ice heat transfer coefficients	$C_h = C_e = 0.00175$	Crocker and Wadhams (1989)
ice/snow/water surf. emissivity	$\varepsilon = 0.97$	Omstedt (1990)
ice total light exctinction coeff.	$\lambda_i = 1.5$ m^{-1}	Gabison (1987)
% of penetrated solar radiation into snow	$i_{0\ snow} = 0.0$	Maykut and Untersteiner (1971)
ice albedo	$\alpha = 0.7$	Perovich (1998)
melting ice albedo	$\alpha = 0.3$	Perovich (1998)
snow albedo	$\alpha = 0.87$	Perovich (1998)
melting snow albedo	$\alpha = 0.77$	Perovich (1998)

2. Determine snow- or rainfall depending on conditions, and apply the isostatic balance equation to test the possible flooding event.
3. Snow metamorphism (steps 4–7 are repeated n times per meteorological forcing timestep).
4. Iterate the surface and the ice–snow interface temperatures from the balance of the heat fluxes and solve the temperature profile through the ice and snow layers (Cranck–Nicholson implicit method).
5. Add internal heating due to penetrating shortwave radiation.
6. Calculate freezing and/or melting processes.
7. Write the output data to a file.

The numerical grid that is used in the model is a 2-dimensional staggered grid in the z–t plane. The grid structure in z-dimension is shown in Fig. 3.

Table 1 presents the main model parameters used in this study. As the model is not coupled with any ocean model it requires the sea freezing date as an input value. Two alternative dates were

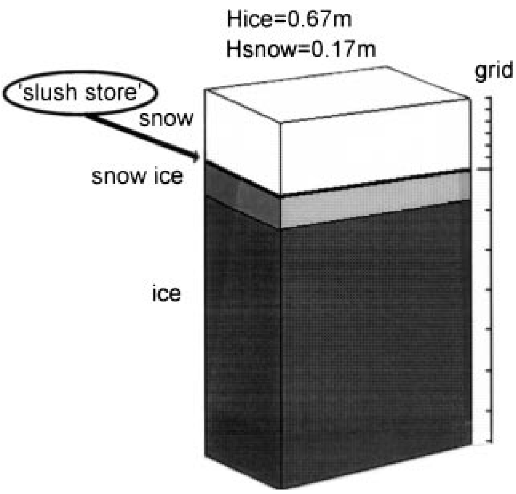

Fig. 3. Schematic illustration of the model layers and grid dimensions.

available in the statistics (Finnish Marine Research, 1982; Kalliosaari and Seinä, 1987; Seinä and Kalliosaari, 1991): "first freezing" and "the formation of permanent ice cover". The latter was chosen for the model as it is better representing the model initial requirements of fast ice cover. The effects of salinity are not taken into consideration other than in defining the freezing point temperature, since salinity is very low at the Kemi ice station.

The model treats ice, snow, snow ice and slush as separate components each having particular variability or value of heat conduction and/or density.

The surface temperature is iterated using the Newton–Rhapson method, and the conductive heat flux on the top surface is calculated from the temperature difference between the 2 uppermost temperature gridpoints. To avoid model instability the uppermost and the third uppermost temperature point is used in snow cover. The oceanic heat flux Q_w is a prescribed value of 5.0 W m^{-2} which is typical for the Baltic Sea (Leppäranta et al., 1997). The turbulent exchange coefficients C_h, C_e in eqs. (3) and (4) depend on air stability, but are kept constant in the model. In calculating the ice–snow interface temperature (eq. (10)), the 2 nearest temperature points in snow and ice are used.

Below the first gridpoint in the ice ($z > 0.1$ m) the radiation is attenuated by the Bouguert–Lambert law and the absorbed radiation flux is used to heat the ice. The radiative energy that would cause internal melting in the ice is taken into account in bottom melting.

The thickness of the snow layer in the model can change for 4 different reasons: (1) snowfall; (2) surface melting of snow; (3) compaction of snow layer; (4) transformation to slush. Wind drift and evaporation–condensation process are neglected in modeled snow mass balance. As discussed in Subsection 2.2, specially wind can be an important factor in reforming the snow cover. However, when averaged over longer time and space scales, its effect on snow thickness can be assumed as minor. Kuusisto (1984) concluded that evaporation from snow cover is negligible in Finland in winter months due to small saturation deficit of air and energy available for evaporation. The model calculates the snow layer thickness from its water equivalent value and its density profile. The threshold value between snow and no-snow conditions in the model is set equal to 3 cm. Meteorological precipitation observations are used to determine the daily snowfall.

The modeled density changes in snow due to compaction are based on Yen (1981) which is discretisized here:

$$\Delta\rho_s = \rho_s C_1 W_s \exp(-C_2\rho_s)\exp(-0.08(T_0 - \mathrm{T}))\Delta t, \tag{13}$$

where ρ_s is snow density in units of g cm^{-3}, C_1 and C_2 are empirical coefficients (Table 1), W_s is the weight of overlying snow in water equivalent [m], and T and T_0 are air and freezing point temperature, respectively.

The compaction is stopped if the density of the snow layer in question reaches 450 kg m^{-3} (Leppäranta, 1983).

The processes that contribute to slush layer water balance were discussed in Subsection 2.3. Of these, flooding, rain- and meltwater percolation, and slush freezing are assumed as the main processes and thus included in the model, while brine expulsion, capillary suction, evaporation and draining into sea or melt ponds are neglected. The contribution of the latter processes to snow ice formation is assumed to be minor, though draining and evaporation may contribute significantly to the water content of slush in the melt season. These processes are also difficult to model properly.

Under significant negative freeboard conditions (in the model an arbitrary snow overload of 20 mm water equivalent is needed for the flooding event to begin), free waterways are assumed and the amount of new slush is calculated from:

$$\Delta h_{\mathrm{slush}} = \frac{\rho_{\mathrm{fw}} W_s - B}{\rho_s + \rho_w - \rho_{\mathrm{slush}}}, \tag{14}$$

where B is the buoyancy of the ice, snow ice and old slush layers:

$$B = h_i(\rho_w - \rho_i) + h_{si}(\rho_w - \rho_{si}) + h_{\mathrm{slush}}(\rho_w - \rho_{\mathrm{slush}}). \tag{15}$$

Here subscripts i, si, s, w, and fw refer to ice, snow ice, snow, sea water and fresh water, respectively.

The contribution of surface meltwater and rain to the slush layer is taken straightforwardly by arbitrarily letting 90% of them contribute to slush layer. The remaining 10% is assumed as a loss term (e.g., held in snowpack and evaporated).

Ice surface temperature is set equal to the freezing point temperature of slush whenever slush is present. The slush layer is assumed to be homogeneous and isothermal until it is totally frozen to snow ice, making it possible to be monitored in the model in a separate "store" (Fig. 3). This means in practice that the model cannot produce "sandwiched" slush layers and it ignores the insulating effect of a frozen snow ice lid on top of the slush layer. The insulation effect of this snow ice lid is generally minor, specially when compared to that of the considerable snow cover which is always needed for slush formation via sea water flooding. In snow ice formation, only the fraction of water in slush need to be frozen.

3.3. *Model testing*

For the testing of the model, both individual winter and longer period comparisons were made against observational data, taken from the coastal Kemi ice station in the northern corner of Bay of Bothnia (Fig. 1). Kemi is a true fast-ice station with long records, and where the sea freezes every year. In the period 1961–90 the observed minimum, mean and maximum ice thicknesses were 0.58 m, 0.76 m and 1.11 m, respectively (Seinä and Peltola, 1991). The measurement site is some 100 m away from the shore (A. Seinä, personal communication).

Two meteorological datasets were used in model testing. First, a dataset from Kemi airport (some 10 km inland from the ice station), which contains mean daily weather data from the normal period 1961–90. Another dataset from the Swedish Meteorological and Hydrological Institute (SMHI) was used later in testing and it proved to be more useful because of better temporal coverage. This dataset was interpolated from the original data of SMHI to a finer grid, and a gridcell representative for Kemi was then finally used in this study. The SMHI dataset contains meteorological data at 3-h intervals for the period 1979–1994. Precipitation data from Kemi Airport was used with both datasets. The missing precipitation observations were recovered by linearly interpolating between the existing observations.

4. Model results

The model results in this study are produced using the SMHI dataset named above. Previously, the model testing has shown that snow plays a crucial rôle in controlling ice growth. It is thus important to model as well as possible the spatial and temporal variation of the snow cover to be able to accurately simulate the natural ice evolution. However the great variability of snow cover is a big problem in modeling work; snow cover is hardly ever evenly distributed in nature. Consequently, snowfall information taken from meteorological precipitation data is often different to ice station snow conditions, not least due to wind drift. This was the main reason why an 11-year averaged mean winter was used in addition to single winters for comparisons between the model and the observations. It was assumed that when averaging over many ice seasons, the differences between modeled and observed snow covers are diminished to a certain extent, and the model consistency can be better evaluated against observations.

4.1. *Normal case*

To produce the *normal* case model results the 11 ice winters 1979–90 in Kemi were simulated with model parameters shown in Table 1. Observational data was obtained for the same period from Finnish Marine Research (1982), Kalliosaari and Seinä (1987), Seinä and Kalliosaari (1991), and observational statistics were calculated. Model results from the normal case, both from individual and mean winters, are presented in Figs. 4–7.

The modeled mean winter 1979–90 in Fig. 4 shows that the total ice thickness evolution is generally well reproduced, but the model slightly overestimates the ice thickness in the early growth season and underestimates it in the late growth season. The maximum mean ice thickness, its timing, and the onset and evolution of the melt season are accurately modeled. The modeled mean date of ice disappearance is 14 May, compared with the observed mean (1979–90) of 17 May.

The modeled mean snow ice thickness shows relatively good overall consistency, but with some overestimation in February and March. As

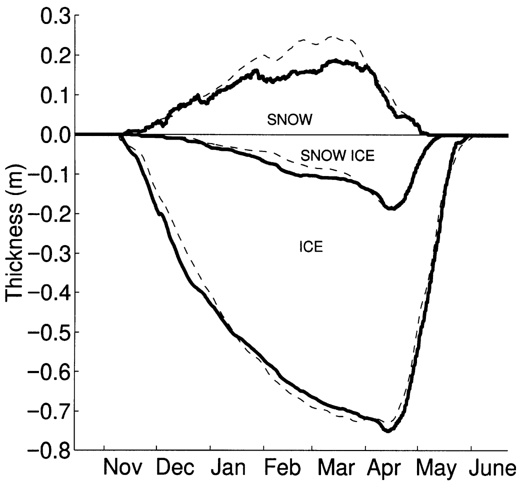

Fig. 4. Modeled mean snow, snow ice and total ice thickness (solid lines) from the ice winter period 1979–90 (normal case, $n = 11$). Dashed lines show corresponding observed mean thickness from the same period.

indicated by the sometimes very long-lasting negative freeboard conditions described in Subsection 2.3 (Fig. 2), it seems that slush formation via flooding has been hampered some, probably due to lack of waterways. The model assumptions of isostatic balance and free waterways were thus not fully valid at Kemi ice station. The modeled rain- and meltwater contribution to snow ice formation, however, agree well with the observed rise in early melt season snow ice thickness.

During the model testing work a puzzling feature in the observed melt seasons was detected, namely that the ratio of snow ice to total ice thickness rose rapidly in many cases, while the new snow ice did not contribute at all to the total ice thickness (the melting season snow ice statistics derived from observations are not fully presented in Fig. 4 due to some missing observations, but this feature can clearly be seen in individual winter observations, Fig. 7). Quite often the last springtime ice thickness observation consisted totally of snow ice. This, at first strange looking phenomenon, was later revealed to be mainly error in ice type classification. The ice observations were made by drilling an ice core and defining the snow ice thickness only by looking at the overall crystal structure (A. Seinä, personal communication). The melt weakened and brine-drained congelation ice has a crystal structure roughly resembling that of snow ice and was mislabeled, despite of its very different origin, as snow ice. A term like "white ice" would be more appropriate for this type of ice and should be used instead of "snow ice", which strictly refers only to ice formed from a mixture of snow and water. The accuracy of the observational snow ice data is consequently dubious in the late melt season.

The maximum mean snow cover thickness is underestimated by the model by some 8 cm, but since there are no data on the snow water equivalent, the real difference remains uncertain. The estimated negative freeboard conditions (Fig. 2) that prevailed for months and hampered some of the flooding probably let a thicker real snow cover accumulate than was modeled. A similar increase in modeled mean snow thickness would require either lower snow bulk density, or different model conditions for water permeability through ice to prevent flooding and to allow higher negative freeboard conditions in the model.

Fig. 5 presents the modeled mean snow water equivalent, slush thickness and snow bulk density. The maximum amount of slush is present in the beginning of February when the snow cover has become heavy enough to trigger flooding, and in April when meltwater and rain contribute greatly to the slush layer. Consequently, 2 slush formation periods, different in their characteristics can be distinguished in model results; the "cold-flooding-period" and the "snowmelt-rain-period". The latter process does not need snow overload or waterways to occur and it can also reduce snow thickness more drastically than flooding does. The full occurrence of the cold-flooding-period at Kemi ice station is however questionable, as just pointed. The snow bulk density shows a growth season average compaction rate of ca. $25\,\mathrm{kg\,m^{-3}}$ $\mathrm{month^{-1}}$ which increases considerably in the melting season. All 3 model output variables presented in Fig. 5 are the type of properties whose field observations are sparse, showing the advantages that the model has in producing that kind of data, though of course lacking direct verification.

The sensitivity of the normal case model results to the magnitude of oceanic heat flux were examined by applying values of 1 and $10\,\mathrm{W\,m^{-2}}$, in contrast to $5\,\mathrm{W\,m^{-2}}$ used in the normal case. Resulting maximum mean total ice thickness were 0.92, 0.78 and 0.63 m for oceanic heat fluxes of 1,

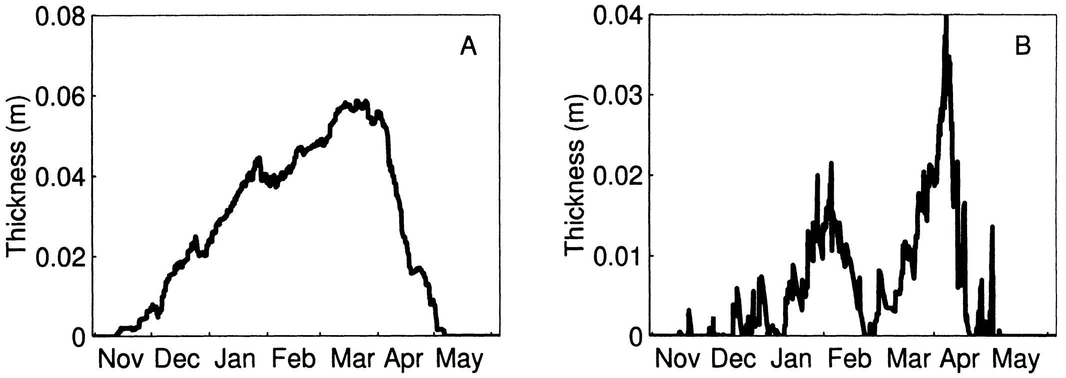

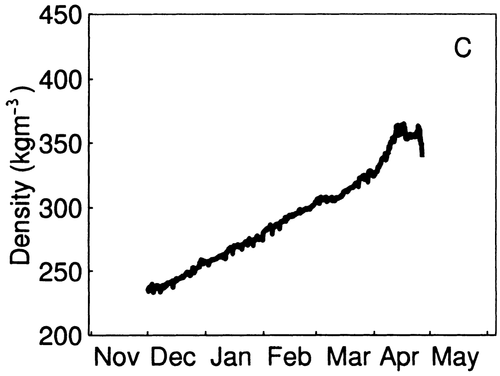

Fig. 5. Modeled mean (A) snow water equivalent, (B) slush layer thickness and (C) snow bulk density from the ice winter period 1979–90 (normal case, $n = 11$).

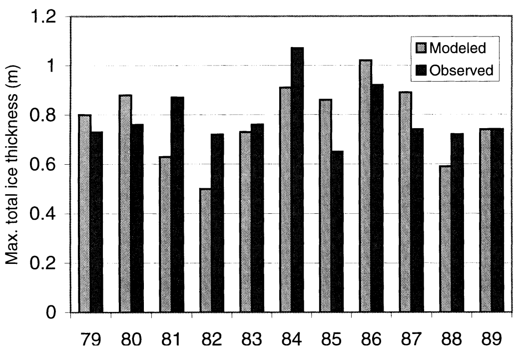

Fig. 6. Modeled and observed maximum total ice thickness in 1979–90.

5 and $10\ \mathrm{W\,m^{-2}}$, respectively. The resulting changes in ice buoyancy slightly affected also snow and snow ice thickness evolution.

Fig. 6 shows the modeled and observed maximum ice thickness for each winter 1979–90. Although the mean maximum ice thickness is well modeled, the variability ΔH ($\Delta H = H_{\mathrm{mod}} - H_{\mathrm{obs}}$) within individual years is quite significant: $\overline{\Delta H} = 1.2$ cm; $\sigma(\Delta H) = 14.9$ cm; $\min(\Delta H) = -21$ cm; $\max(\Delta H) = 24$ cm. More detailed model results from 4 individual ice winters 1985–89 are shown in Fig. 7. They sum up the modeling problem well, where a closer study indicates that the individual winters seem to be rather realistically but more or less accurately reproduced by the model and its forcing. The dissimilarities are mainly connected to (sometimes large) differences between observed and modeled snow cover and to somewhat wrong model assumptions for the local isostatic conditions. The next significant factor contributing to discrepancies may be varying oceanic heat flux. In contrast to snow cover modeling difficulties with the individual winters, the averaging of the model results over many seasons brought the observed and modeled snow covers much closer together, and the physical

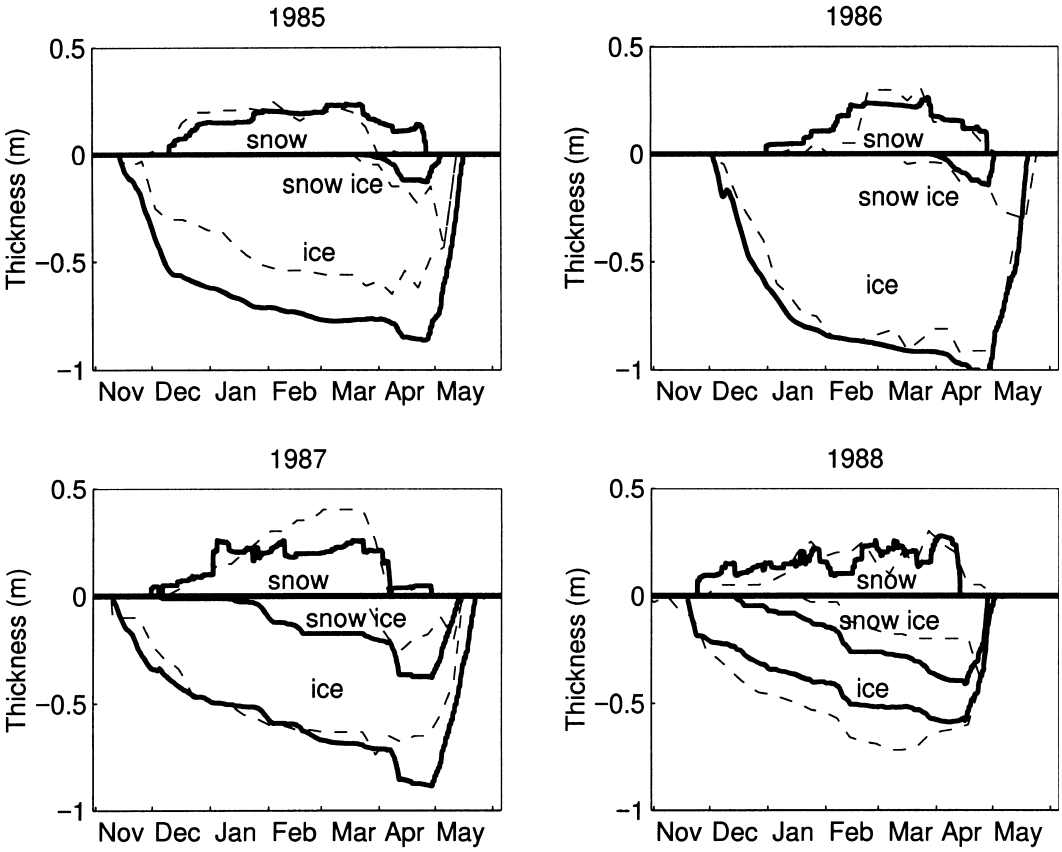

Fig. 7. Modeled snow, snow ice and total ice thickness (solid lines) from the ice winters 1985–89 (normal case). Dashed lines show corresponding observed ice, snow ice and snow thickness.

consistency of the whole model is thus somewhat easier to see.

Ice thickness evolution is especially sensitive to the timing and amount of the snowfall in the early ice season. This is illustrated (Fig. 7) by winter 1988 where this is the main cause of the difference between modeled and observed ice evolution. In winter 1985, the model cannot produce the delayed real ice formation and overestimates the early growth. Winter 1986 is quite well modeled despite the discrepancy in snow cover timing. Here the thicker grown ice is less sensitive to snow cover than thin ice would be. In winter 1987, negative freeboards, which the model did not allow, seemed to prevail for long periods. This resulted in the model producing too much snow ice too early. A cold period interrupting the melt season has produced the modeled snow ice peak in April.

4.2. Sea ice sensitivity to changes in precipitation rate

The SMHI dataset at Kemi was assumed as representative forcing to study generally the northern Baltic sea ice sensitivity to changes in precipitation rate. The forcing precipitation was varied in the model from 0.1 to 1.9 times (in 0.15 intervals) the normal precipitation rate over the period 1979–90. The precipitation pattern was held similar, only the magnitude was changed. Then 13 mean winters, each having a different precipitation magnitude, were produced in a similar way to normal case in Subsection 4.1. The result of the sensitivity study is shown in Fig. 8.

The results indicate that increased snowfall does not lead to any significant change in mean maximum total ice thickness in period 1979–90; it

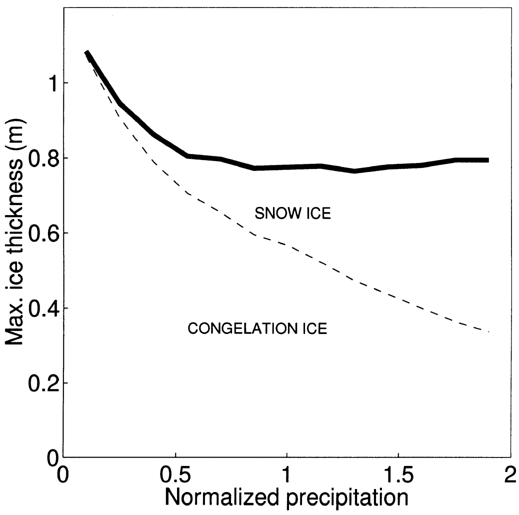

Fig. 8. Modeled mean maximum total ice thickness and corresponding snow ice concentration as a function of changing precipitation rate (normalized, i.e., 1.0 refers to unchanged precipitation, 2.0 to doubled, etc.).

only increases the thickness of snow ice. The increased thermal insulation effect of snow is balanced by enhanced snow ice formation. The effect of increased snowfall on ice thickness within individual winters may, however, depend on the timing and absolute amount of snowfall in that particular winter. The mean maximum thickness of snow can remain quite unchanged although precipitation increases, since extra snow later in the ice season contributes mainly to slush and snow ice formation, and as ice buoyancy does not increase significantly.

A decrease in precipitation rate does not affect the maximum total ice thickness either, until a reduction of more than 50% is applied. Then the thickness of snow ice becomes minor and the decrease in the thermal insulation of snow cover leads to significant ice thickening.

These model results show that the mean maximum ice thickness is not very sensitive to changes in the precipitation rate, although the amount of snow ice is. When compared to the results of Leppäranta (1983) it seems that the effect of increased precipitation, and thus greater snow ice formation, to the total ice thickness is not as big as he expected. Leppäranta (1983) neglected the freezing of the slush in his model, which here, together with the thermal buffering effect of the slush, turns to be an important feature, reducing congelation ice growth drastically. The model results presented here are sensitive to some model assumptions, i.e., to the relative importance of the different slush formation processes, the value of oceanic heat flux as well as the amount of latent heat required for slush freezing (i.e. to the water-soaked snow density).

4.3. Neglecting snow ice formation in the sea ice model

To study the importance of applying snow ice physics in sea ice models, the model was run for the normal case (Subsection 4.1), but no flooding or slush and snow ice formation was allowed and snow was allowed to accumulate freely on the ice surface. Fig. 9 shows the difference between the model runs (mean winter 1979–90) with and without snow ice formation.

Ignoring snow ice formation reduces total ice thickness by some 20 cm (ca. 25%), partly due to a great increase in snow cover thermal insulation, but mainly due to missing snow ice formation. This model example shows the importance of

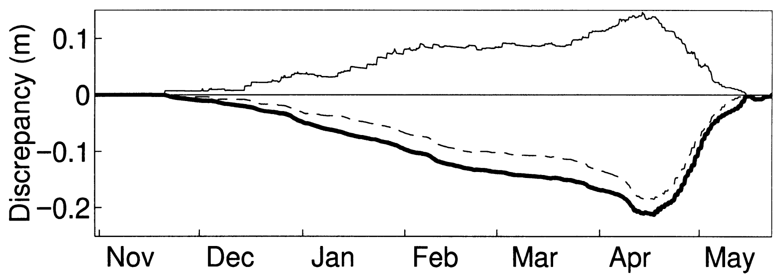

Fig. 9. Difference produced in the model normal case (mean winter) if snow ice formation is neglected ($h_{\text{no snow ice}} - h_{\text{normal case}}$). Thin line refer to snow, dashed line to snow ice, and thick line to total ice thickness.

including at least some snow ice physics into models dealing with the seasonal sea ice zone, where the thickness and thermal insulation effect of snow can easily be exaggerated, and the balancing effect of snow ice neglected if no transformation into slush and snow ice is allowed.

5. Discussion and conclusions

The main objectives of this work were to discuss the role and importance of snow in sea ice thickness evolution and to produce a 1-dimensional numerical sea ice thermodynamic model that includes more detailed and physically realistic handling of snow cover and snow ice formation.

11 ice winters (1979–90) at the Kemi fast ice station were simulated and the modeled mean winter of that period showed generally good consistency with total ice thickness observations. The most pronounced uncertainities in the model was found to be connected with the slush formation processes and snow density. These were probably the main causes for the discrepancy in snow and snow ice simulations. Observations indicated that thicker snow cover could be accumulated on the ice than the model allowed, and similarly less snow was maybe turned into slush. 3 different slush formation processes (flooding, rain- and meltwater percolation) were assumed in the model, but it seemed that specially one of these, namely flooding, was not fully present at Kemi ice station, as the negative freeboard estimates (Fig. 2) also signalized. Kemi sea ice seemed to be able to remain impermeable to sea water for quite long time. This suggests that the model may overestimate slush formation in a thick fast ice zone where the ice is more impermeable for flooding. Moving more offshore, cracks and ice floes should become more common and the isostatic assumption is supposed to be generally valid there (Adolphs, 1998). The rigorous justification of the model assumptions on slush water balance is difficult because no observations on slush layer thickness and water content are presently available.

The early melt season snow ice formation due to rain- and meltwater was well reproduced. The rapidly rising late melt season snow ice concentration in the observations (Finnish Marine Research, 1982; Kalliosaari and Seinä, 1987; Seinä and Kalliosaari, 1991) was indentified mostly as an error in ice type classification.

The modeled snow cover thermodynamics, taking account of the effects of the changing density profile (caused by compaction), gave realistic and sound results. The estimates that the model produced for on-ice snow water equivalent and snow density evolution are also rarely observed parameters in the field. Two separate slush formation periods, one due to flooding and one due to meltwater and rain, were distinguished in the model results. The presence of the former at Kemi ice station is however somewhat dubious.

As the most uncertain model parameters were mainly connected with slush formation (flooding conditions, amount of compaction in water-soaked snow, slush density and salinity and the thermal effect of slush on congelation ice growth), some field studies connected to slush and snow ice physics in the Baltic Sea could reveal a lot of new valuable information for future model development and refinement. For example, the water permeability in ice could be further modeled as a function of ice temperature, salinity, thickness, etc.

With the main assumption that the isostatic balance conditions generally exist in the northern Baltic Sea, away from the very coastal fast ice zone, the model was used to study northern Baltic sea ice sensitivity to changes in winter precipitation. This sensitivity test showed that maximum total ice thickness is not very sensitive to an increase or decrease in wintertime precipitation while the relative amount of snow ice is. The decreased congelation ice growth due to thermal buffering of slush and insulation of snow cover is balanced by increased snow ice formation. If no contribution from snow ice is taken into account in the model, the produced error in maximum total ice thickness showed to be considerable (ca. 25%). This indicates that it is important to include at least some snow ice physics in ice models dealing with the seasonal sea ice zone.

6. Acknowledgements

I thank Matti Leppäranta, Jari Haapala, Mats Granskog, John Moore and the two anonymous reviewers for reading the manuscript and constructively commenting on it. This work is part of the project: “Modeling the long term variability of the Baltic Sea” supported by the Academy of Finland, which is gratefully acknowledged. I thank also the Swedish Meteorological and Hydrological Institute (SMHI) and the Finnish Meteorological Institute (FMI) for providing the Baltic Sea meteorological database for this study.

REFERENCES

Ackley, S. F. 1986. Sea-ice pressure ridge microbial communities. *Antarctic Journal of the United States* **21**, 172–174.

Ackley, S. F., Lange, M. A. and Wadhams, P. 1990. Snow cover effects on Antarctic sea ice thickness. In: *Sea ice properties and processes* (eds. Ackley, S. F. and Weeks, W. F.). US Army Cold Regions Research and Engineering Laboratory, Monograph 90–1, Hanover, NH, USA, 16–22.

Adolphs, U. 1998. Ice thickness variability, isostatic balance and potential for snow ice formation on ice floes in the south polar Pacific Ocean. *J. Geophys. Res.* **103**, C11, 24675–24691.

Crocker, G. B. and Wadhams, P. 1989. Modelling Antarctic fast-ice growth. *J. Glaciol.* **35**, 119, 3–8.

Eicken, H. and Lange, M. A. 1989. Development and properties of sea ice in the coastal regime of the southeastern Weddell Sea. *J. Geophys. Res.* **94**, C6, 8193–8206.

Eicken, H., Lange, M. A., Hubberten, H. W. and Wadhams, P. 1994. Characteristics and distribution patterns of snow and meteoric ice in the Weddell Sea and their contributions to the mass balance of sea ice. *Ann. Geophys.* **12**, 80–93.

Eicken, H., Fischer, H. and Lemke, P. 1995. Effects of the snow cover on Antarctic sea ice and potential modulation of its response to climate change. *Ann. Glaciol.* **21**, 369–376.

Fichefet, T. and Morales Maqueda, M. A. 1997. Sensitivity of a global sea ice model to the treatment of ice thermodynamics and dynamics. *J. Geoph. Res.* **102**, C6, 12609–12646.

Finnish Marine Research (anonymous). 1982. Ice winters 1976–1980 along the Finnish coast. *Finnish Marine Research* **249**, p. 46.

Gabison, R. 1987. A thermodynamic model of the formation, growth, and decay of first-year sea ice. *J. Glaciol.* **33**, 113, 105–119.

Gow, A. J. and Govoni, J. W. 1983. *Ice growth on Post Pond, 1973–1982*. US Army Cold Regions Research and Engineering Laboratory, Report 83–4, Hanover, NH, USA.

Granberg, H. B. 1998. Snow cover on sea ice. In: *Physics of ice-covered seas* (ed. M. Leppäranta). Helsinki University Printing House, 605–650.

Grenfell, T. C. and Maykut, G. A. 1977. The optical properties of ice and snow in the Arctic basin. *J. Glaciol.* **18**, 80, 445–463.

Iqbal, M. 1983. *An introduction to solar radiation*. Academic Press, 390 pp.

Kalliosaari, S. and Seinä, A. 1987. Ice winters 1981–85 along the Finnish coast. *Finnish Marine Research* **254**, 1–63.

Kuusisto, E. 1984. *Snow accumulation and snowmelt in Finland*. Publications of the water research institute, 55, National board of waters, Helsinki, Finland.

Lange, M. A., Schlosser, P., Ackley, S. F., Wadhams, P. and Dieckmann, G. S. 1990. δO^{18} concentrations in sea ice of the Weddell Sea, Antarctica. *J. Glaciol.* **36**, 124, 315–323.

Leppäranta, M. 1983. A growth model for black ice, snow ice and snow thickness in subarctic basins. *Nordic Hydrology* **14**, 2, 59–70.

Leppäranta, M., Shirasawa, K. and Saloranta T. M. 1997. On the oceanic heat flux and ice thickness. In: *Proceedings of the 12th International Symposium on Okhotsk Sea and Sea Ice, 2–5 February 1997*. Okhotsk Sea and Cold Research Association, Hokkaido, Japan, 154–159.

Male, D. H. 1980. The seasonal snowcover. In: *Dynamics of ice and snow masses* (ed. Colbeck, S. C). Academic Press, 305–393.

Maykut, G. A. and Untersteiner, N. 1971. Some results from a time-dependent thermodynamic model of sea ice. *J. Geoph. Res.* **76**, 1550–1575.

Omstedt, A. 1990. A coupled one-dimensional sea ice–ocean model applied to a semi-enclosed basin. *Tellus* **42A**, 568–582.

Palosuo, E. 1963. The Gulf of Bothnia in winter (II). Freezing and ice forms. *Merentutkimuslaitoksen Julkaisu* **209**. Finnish Institute of Marine Research, Helsinki.

Palosuo, E. 1965. Frozen slush on lake ice. *Geophysica* **9**, 131–147.

Perovich, D. K. 1998. The optical properties of sea ice. In: *Physics of ice-covered seas* (ed. M. Leppäranta). Helsinki University Printing House, 195–230.

Pfeffer, T., Illangasekare, T. H. and Meier, M. F. 1990. Analysis and modeling of melt-water refreezing in dry snow. *J. Glaciol.* **36**, 123, 238–246.

Reed, R. K. 1977. On estimating insolation over the ocean. *J. Phys. Oceanogr.* **7**, 482–485.

Röthlisberger, H. 1983. Snow and slush on floating lake ice. *Ann. Glaciol.* **4**, 236–240.

Seinä, A. and Kalliosaari, S. 1991. Ice winters 1986–1990 along the Finnish coast. *Finnish Marine Research* **259**, 3–61.

Seinä, A. and Peltola, J. 1991. Duration of the ice season and statistics of fast ice thickness along the Finnish coast 1961–1990. *Finnish Marine Research* **258**, p. 29.

Semtner, A. J. 1976. A model for the thermodynamic growth of sea ice in numerical investigations of climate. *J. Phys. Oceanogr*. **6**, 379–389.

Szilder, K. and Lozowski, E. P. 1989. A time-dependent thermodynamic model of the build-up of sea-ice platforms. *J. Glaciol*. **35**, 120, 169–178.

Weeks, W. F. 1998. Growth conditions and the structure and properties of sea ice. In: *Physics of ice-covered seas* (ed. M. Leppäranta). Helsinki University Printing House, 25–104.

Yen, Y. 1981. *Review of thermal properties of snow, ice and sea ice*. US Army Cold Regions Research and Engineering Laboratory, Report 81–10, Hanover, NH, USA.